ELSEVIER

Coordination Chemistry Reviews
219–221 (2001) 283–310

COORDINATION CHEMISTRY REVIEWS

www.elsevier.com/locate/ccr

Silver vanadium oxides and related battery applications

Kenneth J. Takeuchi [a,*1], Amy C. Marschilok [a], Steven M. Davis [b], Randolph A. Leising [b], Esther S. Takeuchi [b,*2]

[a] *Department of Chemistry, SUNY at Buffalo, Buffalo, NY 14260, USA*
[b] *Wilson Greatbatch Ltd., 10000 Wehrle Drive, Clarence, NY 14031, USA*

Received 24 August 2000; received in revised form 2 November 2000; accepted 15 November 2000

Dedicated to A.B.P. Lever on the occasion of his 65th birthday

Contents

Abbreviations: Ah, ampere hours, a current of 1 A delivered for 1 h; C rate, charge or discharge rate for a battery necessary to exhaust the rated capacity of the battery in 1 h; DSC, differential scanning calorimetry; DTA, differential thermal analysis; DTG, differential thermal gravimetry; EMF, electromotive force; ESR, electron spin resonance; FT-IR, Fourier transform infrared spectroscopy; HREM, high resolution electron microscopy; TGA, thermal gravimetric analysis; TEM, transmission electron microscopy; SMEA, surface micro-area element analysis; SVO, silver vanadium oxide; Wh, watt hours, energy of 1 W delivered for 1 h; XRD, X-ray diffractometry.

[1] * Corresponding author. Tel.: +1-716-6456800; fax: +1-716-6456963; e-mail: takeuchi@nsm.buffalo.edu

[2] * Corresponding author. Tel.: +1-716-759-5358; fax: +1-716-759-5480.

PII: S0010-8545(01)00340-X

Abstract

This review contains references from journals, proceedings volumes, and patents involving the preparation, characterization, reactivity, and battery applications of materials containing silver, vanadium, and oxygen, hereafter referred to as silver vanadium oxide (SVO). SVO has been a subject of regular study for a number of years, with earlier reports involving the synthesis and characterization of the various phases of SVO. However, with the relatively recent discovery of SVO as an important electrode material in batteries, the number of publications and patents involving the preparation, structure, reactivity and related battery applications of SVO has increased markedly. In light of this recent increase in research activity involving SVO and its related battery applications, this review is a timely examination of this exciting and growing area of research.

Keywords: Silver vanadium oxides; Battery applications; Synthesis and characterization

1. Introduction

This review contains references from journals, proceedings volumes, and patents involving the preparation, characterization, reactivity and battery applications of materials containing silver, vanadium, and oxygen, hereafter referred to as SVO. For the purpose of this review, the term SVO encompasses the general category of materials containing silver, vanadium, and oxygen in a number of stoichiometric and non-stoichiometric ratios. The study of SVO has a long history, with the earlier reports involving the synthesis and characterization of the various phases of SVO. However, with the relatively recent discovery of SVO as an important electrode material in batteries, the number of publications and patents involving the preparation, structure, reactivity and related battery applications of SVO has increased markedly. In light of this recent increase in research activity involving SVO and its related battery applications, this review is a timely examination of this exciting and growing area of research.

2. Chemical studies of silver vanadium oxide

For the purposes of this review, the chemical studies of SVO are divided into four major categories: the synthesis and characterization of SVO, the multiple phases of SVO, the structural analyses of various phases of SVO, and the chemical reactivity that SVO can display towards other substances. A striking observation from the numerous chemical studies of SVO is the variety of phases readily available for these materials and the non-stoichiometric nature of many of the phases. These materials show a very rich chemistry, where variations in reaction conditions, starting materials, and reagent stoichiometries can result in a wealth of products which are subtly different in some aspects and very different in other properties.

Furthermore, the variety of oxidation states available to the silver and vanadium components of SVO suggest that these materials are ideally suited for electron transfer applications, specifically oxidation catalysis and battery applications. It is logical that the development of SVO as a battery electrode material is contemporary with a number of the studies involving SVO as a solid state oxidation catalyst.

2.1. Synthesis and characterization of silver vanadium oxide and related materials

In this section, publications which focus primarily on aspects of synthesis or characterization of solids containing silver, vanadium, and oxygen will be reviewed. Only the aspects of the publications that involve SVO will be discussed and within each section, the publications will be reviewed in chronological order.

Some of the earliest published work on SVO compounds was completed by Britton and Robinson in 1930 [1]. Forward and reverse titrations of aqueous silver nitrate solutions with sodium vanadate solutions were conducted, using silver electrodes. Evidence was observed for the existence of only the 3:1, 2:1 and 1:1 vanadates of silver. During the course of these titrations, vanadates of silver of various Ag:V ratios were formed as precipitates, with the 3:1 and 1:1 precipitates being orange in color and the 2:1 precipitate being light yellow. The solubility products of the vanadates were calculated, ranging from 1×10^{-24} for the 3:1 compound to 2×10^{-14} for the 2:1 silver vanadate to 5×10^{-7} for the 1:1 compound.

Following up on this work in 1933, Briton and Robinson prepared $AgVO_3$, $Ag_4V_2O_7$, and Ag_3VO_4 by various precipitation methods from cold $AgNO_3$/alkali vanadate solutions [2]. Contrary to their earlier report, where all solutions were boiled prior to precipitation, Briton and Robinsion prepared a variety of silver vanadates as precipitates without boiling. It was noted in this report that the boiling or aging of the sodium vanadate solutions was crucial to the preparation of well defined vanadate solutions and the resulting silver vanadate precipitates. Omission of boiling or aging resulted in more complex silver vanadate precipitates in terms of composition, color and physical appearance. In addition, silver electrodes were used to generate EMF as a function of sodium vanadate equivalents plots for various silver cation concentrations as well as pH as a function of sodium vanadate equivalents plots for various types of sodium vanadate solutions.

In 1967, Lukacs et al. thermally treated mixtures of $AgVO_3$ and V_2O_5 where the temperatures ranged from 450 to 600°C [3]. Two phases of $Ag_xV_m^{4+}V_n^{5+}O_y$ were initially obtained: phase I, where $0.29 < x < 0.43$, $0.32 < m < 0.44$, $1.56 < n < 1.68$, $4.96 < y < 5.05$ and phase IIA, where $0.80 < x < 0.99$, $0.06 < m < 0.20$, $1.90 < n < 1.94$, $5.32 < y < 5.46$. This mixture was treated with HNO_3 and a third phase of $Ag_xV_m^{4+}V_n^{5+}O_y$ was obtained: phase IIB, where $0.67 < x < 0.77$, $0.05 < m < 0.09$, $1.91 < n < 1.95$, $5.22 < y < 5.36$. Notably, phase IIB was V^{4+} deficient, possibly due to the oxidizing character of HNO_3. The mixtures were characterized via TGA, IR spectroscopy, X-ray diffraction, and redox titrations.

In 1969, Casalot prepared SVO bronzes of the general formula $Ag_xV_2O_5$, and conducted magnetic susceptibility measurements for bronzes where $0.72 < x < 0.80$

[4]. In addition, energies of activation were reported at 125 and 400 K for four species within the range of $0.70 < x < 0.80$. A correlation between structure and physical properties for $Ag_xV_2O_5$ was described.

In 1978, Chakraverty et al. investigated the low temperature (below 100 K) specific heat and magnetic susceptibility of a crystalline $Ag_{0.33}V_2O_5$ β-vanadium bronze [5]. The material was formed by heating a mixture of Ag_2CO_3 and V_2O_5 in a platinum dish for 30 h at 720°C, cooling at 0.6°C min^{-1} to about 650°C, and then cooling at 2–3°C min^{-1} to room temperature. The species was treated with hot 6 N aqueous NH_3 and then washed, dried, and ground into a fine powder. A linear relationship was observed between specific heat and T^2, and also between the inverse of magnetic susceptibility and T. These results were then rationalized using a bipolaron model.

In 1989 Znadi et al. synthesized monoclinic β-phase SVO via a sol gel process involving V_2O_5 xerogels [6]. V_2O_5 gels were formed via acidification of a vanadium salt solution by passing the solution through an ion exchange column. After gelation, the resulting V_2O_5 fibers looked like entangled flat ribbons about 1000 Å long, 100 Å wide, and 10 Å thick. The V_2O_5 gels were spread as a thin layer (about 0.04 mm thick) and dried to form a thin xerogel. Intercalation of silver cations was obtained by directly immersing the xerogel film into a solution 0.1 M in silver cation for a few minutes. The intercalated compound obtained was $Ag_{0.36}V_2O_5{\cdot}1.17H_2O$, with a d-spacing of 10.9 Å. By dehydration and heating of the intercalated xerogel, the bronze $Ag_{0.36}V_2O_5$ was formed. X-ray powder diffraction coupled with thermogravimetric and differential thermal analysis was used to follow the initial formation of the material at 320°C through an intermediate around 360°C and finally to a single phase material at 500°C, which displayed x-ray diffraction peaks similar to a material formed by Casalot and Pouchard [7] (vide infra).

2.2. Multiple phases of silver vanadium oxide

Materials containing various amounts of silver, vanadium, and oxygen can form a number of phases, depending on reaction conditions and material stoichiometry. In this section, publications which feature discussions of the various phases of SVO will be described.

In 1964, Deschanvres and Raveau reported preparation of three phases of SVOs, obtained through the reaction of silver with vanadium oxide (V_2O_5) in the presence of a vacuum or air [8]. Distinct phases and phase mixtures were defined for $Ag_xV_2O_5$ over several ranges of x. From $0.17 < x < 0.45$ a homogeneous β phase was observed. A homogeneous δ phase was observed from $0.6 < x < 0.8$, and a bi-phasic region of β plus δ occurred when $0.45 < x < 0.6$. For reactions in the presence of air, an ε phase was generated, homogeneous from $1 < x < 1.15$. In the case where $x = 1$, the product from the air reaction was described as $Ag_2V_4O_{11}$, observed as shiny clear blue crystals. At still higher levels of silver $AgVO_3$ was obtained, consistent with complete oxidation of V. Finally, it was noted that the δ phase undergoes a complex air oxidation at 500°C, yielding a mixture of β and ε

phases. This oxidation may explain why the δ phase is difficult to isolate in the presence of air.

In 1966, Fleury et al. used thermal analysis on the $Ag_2O–V_2O_5$ system to construct a phase diagram from the combination of the two oxides in five distinct ratios 1/7, 1/2, 1/1, 2/1, and 3/1 [9]. The first four compounds, AgV_7O_{18}, $Ag_2V_4O_{11}$, $AgVO_3$, and $Ag_4V_2O_7$, displayed melting points which ranged from 732°C for AgV_7O_{18} to 392°C for $Ag_4V_2O_7$, where the decrease in melting point corresponded to an increase in Ag:V ratio. It was noted that the thermal analyses were conducted under flowing oxygen in order to avoid the in-situ formation of bronzes which can complicate the analyses.

In 1967 Casalot and Pouchard prepared a phase diagram for the $Ag_2O–V_2O_5–VO_2$ system through the reaction of silver with V_2O_5 and $AgVO_3$ with V_2O_5 [7]. Three successive phases of $Ag_xV_2O_5$ were prepared via the reaction of silver with V_2O_5 in a Vycor tube at 600°C (two thermal treatments of 24 h each, followed by crushing and tempering): an α phase from $0 < x < 0.01$ consisting of a solid solution of Ag^+ ions in V_2O_5, a monoclinic β phase from $0.29 < x < 0.41$, and a δ phase from $0.67 < x < 0.86$. The melting points of the phases were determined: α phase m.p. = 672°C, β phase m.p. = 715°C, δ phase m.p. = 690°C. The α and β phases were stable with melting, while upon melting and subsequent cooling, the δ phase transformed into a mixture of β phase, VO_2, and $AgVO_3$. At x values between phases both adjoining phases were observed. Four successive phases were prepared via the reaction of $AgVO_3$ with V_2O_5 under an oxygen atmosphere. The reaction temperatures ranged from 350°C for a V:Ag ratio = 1 to 640°C for a V:Ag ratio = 19. Four phases were identified. Phase I was the β phase of $AgVO_3$. Phase II corresponded to an 'oxygen deficient ' phase of $Ag_2V_4O_{11-e}$, where $e = 0.16$ when the pressure of oxygen = 1 atm and the temperature = 500°C. The value of e decreased with increasing oxygen pressure. Phase III coexisted with phase IV, where phase III was described by the $Ag_{1+x}V_3O_8$. Phase III also melted with decomposition to phases II and IV. Phase IV appeared when the V:Ag ratio was greater than 2.5. Notably, for V:Ag = 6, phase IV was pure and appeared to be the β phase of $Ag_{0.33}V_2O_5$.

Casalot et al. continued their studies of SVO with their report in 1968 of the magnetic susceptibility and conductivity as a function of temperature for the α, β, and δ phases of $Ag_xV_2O_5$ [10]. All three phases exhibited similar Curie temperatures, and followed the Curie–Weiss law, with the δ phase deviating below 220 K. In addition, conductivity was measured as a function of temperature for the three phases, and energies of activation were also reported.

In 1976, Scholtens measured the diffusion constants of silver in $Ag_xV_2O_5$ as a function of x in a temperature range from 200 to 450°C [11]. $Ag_xV_2O_5$ was prepared in three ways: Silver + V_2O_5 at 650°C, $Ag_2CO_3 + V_2O_4 + V_2O_5$ at 650°C, and $AgI + V_2O_5$ above 300°C. The silver diffusion constant (D_{Ag+}) for $Ag_xV_2O_5$ varied with x: for $x = 0.30$, $D_{Ag+} = 10^{-13}$, while for $x = 0.70$, $D_{Ag+} = 10^{-16}$. When $x = 0.30$, $Ag_xV_2O_5$ is in the β phase, while when $x = 0.70$, $Ag_xV_2O_5$ is in the δ phase. Since the tunnels in both phases were almost the same size, the authors proposed that diffusion was faster in the β phase because there were more unoccupied energetically-equivalent sites.

Ten years after the study by Fleury [9] (vide supra), Volkov et al. reported in 1976 an equilibrium diagram of the V_2O_5–$AgVO_3$ system [12]. Mixtures of V_2O_5 with $AgVO_3$ were heated for 200 h in an atmosphere of air where the temperatures ranged from 400 to 450°C. The mixtures were ground periodically. Chemical analysis and X-ray diffraction measurements of the products revealed three materials: β-$Ag_xV_{12}O_{30}$ ($1.7 < x < 2.0$), γ-$Ag_{1.12}V_3O_{7.8}$, and ε-$Ag_2V_4O_{10.85}$ which were characterized via X-ray diffraction. Notably, the compositions of the products were functions of the oxygen reaction pressure, so it is important to note the specific equilibrium conditions when a equilibrium phase diagram of V_2O_5-$AgVO_3$ is constructed (Fig. 1).

Nine years after the Volkov study, Wenda et al. investigated the V_2O_5–Ag_2O system in 1985 [13]. Powdered samples of V_2O_5 and Ag_2O were mixed and heated under air in a quartz tube at temperatures ranging from 380 to 640°C, with a variety of reaction times. Many of the materials were rapidly cooled to liquid nitrogen temperatures from the reaction temperatures, while a few samples were slowly cooled in order to obtain the best possible equilibration. The materials were characterized by DTA, TGA, and X-ray powder diffractometry. Seven phases were observed including V_2O_5, solid Ag or Ag_2O in V_2O_5, β-$Ag_{0.30}V_{1.7}O_{4.25}$, $Ag_2V_4O_{11}$, β-$AgVO_3$, Ag_3VO_4 and Ag. A phase diagram was presented in partial agreement with both the work of Fleury [9] and Volkov [12]. However, unlike Fleury, the thermal transitions from α to β (372°C) and β to γ (473°C) phase were not observed, the shape of the liquidus from 12–35 mol% Ag_2O was different, and thermal effects at 400°C for samples with more than 66 mol% Ag_2O were not observed.

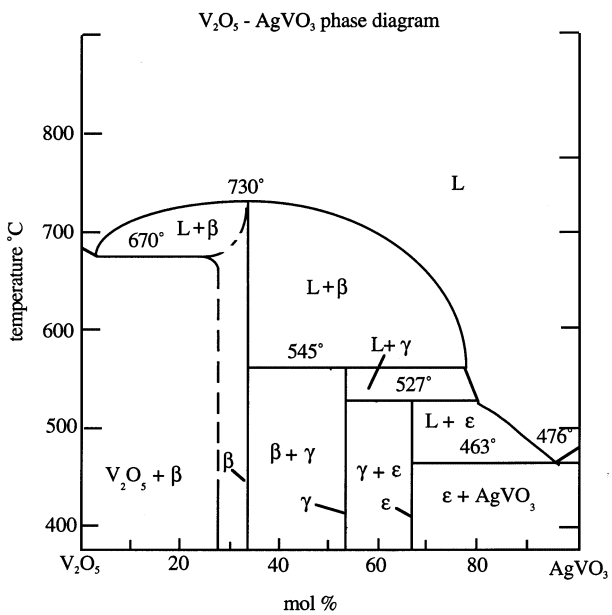

Fig. 1. The $AgVO_3$–V_2O_5 phase diagram [12].

Also in 1985, Ivanova and Dmitriev studied phase equilibrium in the Ag_2O–TeO_2–V_2O_5 system using DTA and X-ray phase analysis [14]. A phase diagram for the system was proposed, and the fields of crystallization for 12 crystalline phases were outlined, including some phases which contained only silver, vanadium, and oxygen.

2.3. Structural studies of silver vanadium oxide

In this section, publications which focus primarily on the structures of materials containing silver, vanadium, and oxygen will be reviewed. Only the aspects of the publications that involve SVO will be discussed.

In 1965, Andersson combined water and V_2O_5 in silver capsules and heated the sealed capsules at temperatures between 300 and 700°C under applied pressures of 2000 atm [15,16], obtaining $Ag_{1-x}V_2O_5$ as blue–black crystals after three days of heating and pressure. The crystals were sometimes rod-shaped and sometimes plate-like. Using X-ray powder diffraction, the crystal was assigned a space group of $C2/m$, and a value for x of ca. 0.32 was determined after least-squares treatment. A monoclinic unit cell was determined, with $a = 11.742$ Å, $b = 3.667$ Å, $c = 8.738$ Å, $\beta = 90.48°$. Two independent vanadium atoms, V_1 and V_2, were resolved, each one having oxygen neighbors at the corners of a distorted trigonal bipyramid. V_1–O distances ranged from 1.42–1.95Å and V_2–O distances ranged from 1.54–2.10 Å. For both V_1 and V_2 there was one further oxygen at the distances of 2.43 and 2.35 Å to complete the distorted octahedron around each V. The silver atom displayed ca. fivefold coordination, with Ag–O distances ranging from 2.48–2.68 Å. The overall structure was described as V_2O_5 layers consisting of double zigzag ribbons of distorted VO_6 octahedra sharing edges and corners (see Fig. 2). Silver ions were positioned between the V_2O_5 layers. Finally, the authors noted similarities and differences between the structure of $Ag_{1-x}V_2O_5$ and the structure of $Na_xTi_4O_8$.

In 1966, Hagenmuller et al. prepared and reported on a series of vanadium bronzes, including $Ag_xV_2O_5$ [17]. Four phases were reported, an orthorhombic α phase from $0 < x < 0.01$, a monoclinic β phase from $0.29 < x < 0.41$, and a monoclinic δ phase from $0.67 < x < 0.86$. Above $x = 0.86$, silver metal and the δ phase were observed. For $x = 0.86$, the parameters of a unit cell were determined, with $a = 11.73 \pm 0.03$ Å, $b = 3.66 \pm 0.02$ Å, $c = 8.75 \pm 0.02$ Å, $\beta = 91°30' \pm 30'$, the space group $= C_{2h}^3$ and $Z = 4$. These cell dimensions are similar to the cell dimensions reported by Andersson for $Ag_{1-x}V_2O_5$ where $x = 0.32$, but the space group differed . Conductivity for the α phase is reported to be on the magnitude of $10^{-3}\ \Omega^{-1}\ cm^{-1}$ ($T = 300$ K), whereas the conductivities of the β and δ phases are reported to be on the order of $10^{0}\ \Omega^{-1}\ cm^{-1}$ ($T = 300$ K).

In 1967, Casalot, Hagenmuller, et al. related the range of phases associated with vanadium bronzes of the general formula $M_xV_2O_5$ (where M = monovalent, divalent, or trivalent metals) to the ionic radius and insertion rate of M [18]. Included in this analysis was the δ phase $Ag_{1-x}V_2O_5$ characterized by Andersson . The structure of this monoclinic $C2/m$ crystal was compared to the structures of five other $M_xV_2O_5$ phase types, namely α, β, γ, α′, and 0 phases. In all cases, the V_2O_5

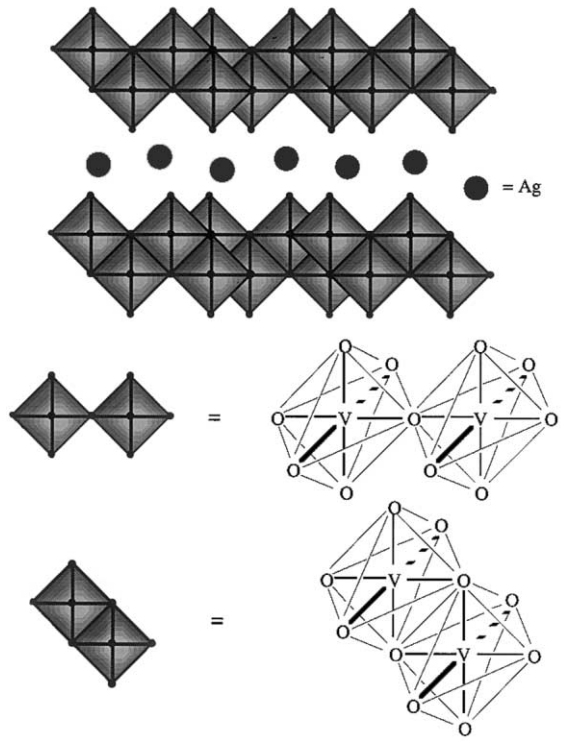

Fig. 2. δ-$Ag_xV_2O_5$, a layered structure of distorted VO_6 octahedra sharing edges and corners (distortions not shown) [15,16].

part of the $M_xV_2O_5$ phases consists of distorted octahedra and bipyramids forming parallel chains arranged two or three dimensionally within the solid. The metal centers are positioned between or among the V_2O_5 chains.

In 1974, Drozdov et al. reported the crystal structure of $Ag_{4-x}V_4O_{12}$ ($x = 1.05$), where the authors noted that the deviation from stoichiometry by the Ag ions destroyed the periodicity of the crystal and complicated the structural analysis [19]. Thus, the Shenk method was used to aid in the structural interpretation. The crystals were supplied to the authors by the Laboratory of Hydrothermal Synthesis at the Institute of Crystallography of the Academy of Sciences of the USSR. The structure is described in terms of V_4O_{12} repeat units, consisting of V octahedra, which form infinite isolated vanadium–oxygen rods ($[V_4O_{12}]_8$). The authors suggest that the infinite rod structures determine the fibrous character of the $Ag_{4-x}V_4O_{12}$ ($x = 1.05$) crystals. The authors also note that infinite isolated vanadium–oxygen rods of $Ag_{4-x}V_4O_{12}$ ($x = 1.05$) are reminiscent of the structural components of other vanadium bronzes; however, in these vanadium bronzes the infinite rods are not isolated but rather are parts of more complex two and three dimensional structures. It is interesting that from the stoichiometry of the title compound, $Ag_{4-x}V_4O_{12}$ ($x = 1.05$), in order to have charge balance, either the charge of at

least one of the Ag ions is more positive than $+1$ or the charge of at least one of the O ions is less negative than -2.

Galy et al. conducted several studies concerning the structure of V_2O_5 and the related structural chemistry of MV_2O_5 phases. In 1986, a refinement of the structure of V_2O_5 was reported, where the structure of V_2O_5 was described as a layered structure, built up from VO_5 square pyramids sharing edges and corners, with V_2O_5 sheets held together via weak vanadium–oxygen interactions (V–O distance = 2.791(3) Å) [20]. This report was important because previous to this report, the VO_5 polyhedra were described as trigonal bipyramids instead of square pyramids. In 1992, structural changes in the structure of V_2O_5 due to metal insertion were investigated and explained [21]. By examining a number of different structural changes due to metal insertion, Galy was able to reason structural changes via S-layer shrinkage, with the extension of the vanadium coordination from five to six, which gave rise to the formation of double layers, characterized in part by quadruple strings of octahedral sharing of edges, and by relative layer displacement, Δ, expressed as a fraction or a unit of the height O_c of an octahedron. Finally, in 1994, Galy et al. investigated the novel silver insertion mode into β-$Ag_xV_2O_5$ tunnel structure, where $0.29 = x = 0.41$[22]. Recalling the study by Casalot and Pouchard (vida supra) regarding the phases of $Ag_xV_2O_5$, Galy et al. were able to confirm the structure of β-$Ag_xV_2O_5$ and rationalize why the value of x in β-$Ag_xV_2O_5$ has been observed to overstep the theoretical boundary limit of β phases ($x = 0.33$). The justification for the large values of x in β-$Ag_xV_2O_5$ came from the realization that Ag could distribute over more sites than previously observed for other metals. From their observations, the authors suggested that the new upper limit for the β phase of $M_xV_2O_5$ was 0.66 instead of 0.33.

In 1999, Zavalij and Whittingham reviewed the structural chemistry of vanadium oxides with open frameworks [23]. Since the Whittingham review includes many topics outside the scope of this review, it will not be discussed here. However, it is mentioned because the Whittingham review has relevance to the Galy studies, especially regarding the structural changes observed with the insertion of silver into the V_2O_5 framework.

In 1993 and 1994, Zandbergen et al. collected high resolution electron microscopy (HREM) data and X-ray powder diffraction data for $Ag_{2-x}V_4O_{11}$ [24,25]. SVO was prepared by the solid state reaction of Ag_2O with V_2O_5 in a 1:2 ratio at 500°C under an oxygen atmosphere for 6 h. Notably, small particles of silver were observed via HREM on the SVO surface, but due to small size and volume fraction, the silver particles could not be observed via X-ray powder diffraction. From this observation the authors suggested the formulation for SVO was more appropriately $Ag_{2-x}V_4O_{11}$ than $Ag_2V_4O_{11}$. However, it was also noted that the value for x was difficult to determine. Two phases were observed via HREM, phase I and phase II. Phase I, the majority phase, was a two-dimensional cell with $a = 0.77$, $c = 0.90$ nm, $\beta = 125°$, which corresponded to a C-centered monoclinic unit cell ($a = 1.53$ nm, $b = 0.360$ nm, $c = 0.95$ nm and $\beta = 125°$). Phase II, differing from phase I only in the stacking along the c^* axis, was a two dimensional cell with $a = 0.77$ nm, $c = 0.72$ nm, $\beta = 102°$, where the authors propose a C-centered

monoclinic cell ($a = 1.53$ nm, $b = 0.36$ nm, $c = 0.76$ nm, and $\beta = 102°$). The authors cautioned that a variation of several degrees in β was observed, even within the same crystal. In addition, the cell dimensions were a function of the sample treatments and beam conditions. Finally, several possible structures of $Ag_{2-x}V_4O_{11}$ are proposed, based on the shifting of V_4O_{11} slabs. The V atoms in these slabs exhibited distorted six coordination, while the Ag ions displayed irregular oxygen coordination.

In 1996, Rozier et al. determined the structure of β-$AgVO_3$, using single crystal X-ray diffraction and compared it to the reported structures of $Ag_2V_4O_{11}$ and δ-$Ag_xV_2O_5$ [26]. A β-$AgVO_3$ powder was prepared by heating a 1:1 mixture of Ag_2O and V_2O_5 in a gold crucible at 420°C for 12 h under a stream of oxygen gas. The mixture was reheated under the same conditions in order to obtain a well crystallized red powder. In order to form single crystals, the β-$AgVO_3$ powder was heated in a gold crucible under an oxygen atmosphere at 500°C for 10 h, cooled to 450°C at a rate of -2°C h^{-1}, then quenched to room temperature. The authors noted that the β phase transformed into the γ phase at 420°C. In addition, the authors noted that the crystals were of poor quality and several different crystals were examined by X-ray diffraction, with the best result reported. The β-$AgVO_3$ crystal was assigned to the monoclinic system, space group *Cm*, and the structure consisted of infinite $[V_4O_{12}]_n$ chains of edge shared VO_6 octahedra where the chains were zigzag in shape and were double. The VO_6 octahedra were distorted, with four different V–O bond lengths ranging from 1.67(4) to 2.44(8) Å. The four silver atoms were distributed in three types of surroundings: the first Ag atom was six coordinate with the bonded oxygen atoms positioned in a weakly distorted octahedron (typical bond distance = 2.43(4) Å); a second and third Ag atom were five coordinate, with the bonded oxygen atoms positioned in a square pyramid, where the Ag–O bonds were similar in magnitude (typical bond distance = 2.40 Å); and the fourth Ag atom was seven coordinate, with the bonded oxygen atoms positioned in a monocapped trigonal prism, where the Ag–O bond lengths ranged from 2.22 to 2.89 Å. Since the fourth Ag atom was positioned in the largest site and the monocapped trigonal prisms shared faces along the [010] direction, the authors proposed that these Ag atoms might be particularly mobile within the crystalline lattice. Finally, due to the strong three dimensional network of V_4O_{16} double chains held together by $Ag1O_6$ octahedra and further interlinked by Ag_2O_5 and Ag_3O_5 square pyramids, the authors proposed that β-$AgVO_3$ can be envisioned structurally as $Ag[Ag_3V_4O_{12}]$, where the Ag^+ is Ag_4. The authors also discussed the structural similarities among β-$AgVO_3$, $Ag_2V_4O_{11}$, and δ-$Ag_xV_4O_{10}$, and proposed possible routes of interconversion via loss of Ag_2O or O (see Fig. 3).

Rozier and Galy followed up on this work in 1997, detailing a proposed sprouting mechanism for the transition of $Ag_2V_4O_{11}$ to $Ag_{1+x}V_3O_8$ via loss of oxygen through $Ag_2V_4O_{11-y}$ [27]. A polycrystalline sample of ε-$Ag_2V_4O_{11}$ was prepared by heating a 1:2 molar mixture of Ag_2O and V_2O_5 in a sealed quartz ampule at 450°C for 10 hours, followed by reheating at 500°C for 10 h. To obtain single crystals of ε-$Ag_2V_4O_{11}$, the polycrystalline sample was heated in a sealed quartz ampule at 560°C for 5 h, cooled at 2°C h^{-1} to 540°C and quenched to room

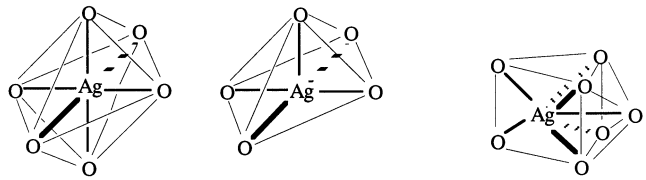

Fig. 3. Four silver environments, octahedral (Ag_1), square pyramidal (Ag_2, Ag_3), and capped trigonal prism (Ag_4) [26].

temperature. Dark blue crystals were obtained along with a brown powder. A crystal was subjected to complete single crystal X-ray analysis and the chemical formula of the crystal was determined as $Ag_{1+x}V_3O_8$ instead of $Ag_2V_4O_{11}$; the space group was determined to be $P2_1/m$. The $[V_3O_8]_n$ chain framework was built around three independent vanadium sites: V_1 exhibited a five coordinate, trigonal bipyramidal coordination environment of oxygen atoms, while V_2 and V_3 exhibited a six coordinate, octahedral coordination environment of oxygen atoms. The Ag^+ ions resided mainly in weakly distorted octahedral sites (typical Ag–O distance = 2.438(8) Å), while some of the Ag^+ ions were in sites described by the authors as having tetrahedral and trigonal prismatic limiting forms. The Ag–O distances in these sites varied from 2.09(1) to 3.30(1) Å. The authors proposed that the electrochemical results of Leising and Takeuchi [28] (vida infra), as well as Tarascon and Garcia Alverado [29] (vida infra) regarding SVO prepared in air or an inert atmosphere could be rationalized if the material prepared under inert atmosphere was $Ag_{1+x}V_3O_8$. Finally, a Ag_2O–V_2O_5–V_2O_4 ternary diagram was proposed and sprouting phenomenon discussed as a possible means of rationalizing an ε-$Ag_2V_4O_{11}$ to $Ag_{1+x}V_3O_8$ transition.

Finally, in 2000, Rozier et al. characterized lithium insertion into V_2O_5 and $Ag_2V_4O_{11}$, using solid state chemistry and X-ray diffraction (XRD) measurements [30]. The starting γ-$Li_xV_2O_5$ was prepared by the solid state reaction between $LiVO_3$ and VO_2. Lithium insertion was accomplished chemically by the following two routes:

$$\gamma\text{-}Li_xV_2O_5 + yC_4H_9Li \rightarrow Li_{x'}V_2O_5 + y/2C_8H_{18}$$

where $x' = x + y$ (with $1 < x' < 3$)

$$\gamma\text{-}Li_xV_2O_5 + y/2Li_2C_2O_4 \rightarrow Li_{x'}V_2O_5 + yCO_2$$

where $x' = x + y$ (with $1 < x' < 3$)

X-ray diffraction measurements made on the $Li_{x'}V_2O_5$ materials suggest that when $x' > 1$ in several phases result, and that the stepped discharge profile obtained during discharge of a Li/V_2O_5 cell results from the demixing of these phases until $LiVO_2$ is obtained. The authors prepared $Ag_2V_4O_{11}$, heated it to melting under vacuum for 5 h, and then cooled the material in order to prepare the oxygen-deficient $Ag_2V_4O_{11-y}$ phase. The authors observed that the oxygen deficient

$Ag_2V_4O_{11-y}$ had an identical X-ray diffraction pattern to that predicted for $Ag_{1+x}V_3O_8$, and thus asserted that electrochemistry associated with oxygen deficient $Ag_2V_4O_{11-y}$ should be interpreted in terms of addition of lithium to $Ag_{1+x}V_3O_8$. Noting that $Ag_{1+x}V_3O_8$ and $Li_{1+x}V_3O_8$ are isostructural, the authors proposed a mechanism where lithium first inserts to create $(Li,Ag)^+_{1+x}V_3O_8$ and then finally $Li_{1+x}V_3O_8$. This mechanism accounts for the similarity in discharge curves between $Ag_{1+x}V_3O_8$ and $Li_{1+x}V_3O_8$. Finally, lithium was inserted into $Ag_{1+x}V_3O_8$ by reacting $Li_2C_2O_4$ with $Ag_{1.2}V_2O_8$; a mixture of $Li_{1+x}V_3O_8$ and silver metal was obtained, consistent with the proposed mechanism.

2.4. Chemical reactivity of silver vanadium oxide

In this section, publications which focus primarily on the chemical reactivity of materials containing silver, vanadium, and oxygen will be reviewed.

In 1967, Raveau investigated some of the chemical reactivities of materials derived from the V_2O_5–Ag_2O system [31]. First, Raveau studied the thermal stability of some of the phases of the V–Ag–O system in vacuo, under an inert atmosphere, and under an oxygen atmosphere. This study provided insight into the interconversion of some of the phases of the V–Ag–O system. For example, β–$Ag_xV_2O_5$ was stable under air or oxygen, but unstable in vacuo, while δ-$Ag_xV_2O_5$ oxidized in air at 500°C to form $Ag_2V_4O_{11}$ and β-$Ag_xV_2O_5$. Further, $Ag_2V_4O_{11-y}$ was formed from the decomposition of $Ag_2V_4O_{11}$ at 450°C in vacuo, and $Ag_2V_4O_{11-y}$ decomposed in vacuo at 550°C into δ-Ag_xV_2O, silver, and oxygen. In addition, $Ag_2V_4O_{11-y}$ was formed from γ-$AgVO_3$ at 450°C while $Ag_2V_4O_{11}$ and $Ag_2V_4O_{11-y}$ were reduced by VO_2 at 500°C to form δ-$Ag_xV_2O_5$. Second, Raveau studied the reaction of gaseous ammonia with δ-$Ag_xV_2O_5$ and liquid ammonia with β- and δ-$Ag_xV_2O_5$. In general, in the presence of humidity, ammonium vanadate and silver were reaction products.

In 1981, Volkov and Andreikov reported on the catalytic properties of SVO compounds in the oxidation of *o*-xylene and napthalene where the reaction temperature ranged from 360 to 420°C [32]. To prepare the catalysts, mixtures of silver nitrate and vanadium oxide in 12 different ratios were fused at 750°C in an atmosphere of air, producing several phases of SVO. X-ray diffraction was used to identify α phase material, $Ag_xV_2O_5$, obtained when silver concentration was low ($0 < x < 0.02$), and β phase material, obtained for $Ag_xV_6O_{15}$ where $0.85 \leqslant x \leqslant 1.0$. Silver vanadates $Ag_{1.2}V_3O_7$(γ) and $Ag_2V_4O_{10.5}$ (ε) as well as the silver metavanadate $AgVO_3$ were also observed. A molar concentration of 20–30 at.% Ag appeared to optimize target oxidation. Notably, the catalysts compositions changed during the course of the catalyses, with the following exceptions: β phase $Ag_xV_6O_{15}$, where the $Ag/Ag+V$ ratio = 0.14, and $AgVO_3$ did not decompose.

In 1983, Van Den Berg et al. conducted a thermal analysis study of V_2O_5, $Ag_{0.35}V_2O_5$, and mixture of 0.35 $Ag + V_2O_5$, using DTA, TGA, DTG measurements and a variety of inert, oxidizing, and reducing atmospheres with a maximum

temperature of 600°C [33]. The authors noted that the presence of silver catalyzes the reduction of vanadium and that mixtures of $0.35Ag + V_2O_5$ displayed initial reduction DTG curves that differ from the initial reduction DTG curves of $Ag_{0.35}V_2O_5$. Further, the second reduction DTG curve of the mixture was similar in appearance to the first reduction DTG curve of $Ag_{0.35}V_2O_5$. These results were rationalized in part by the inhomogeneous distribution of silver in the mixture, which became more homogeneous after the first reduction.

In 1991, Zhang et al. prepared vanadium oxide catalysts by combining silver nitrate and ammonium metavanadate in aqueous solution, evaporating the solution, and then calcining the resulting material at 450°C for nine hours [34]. The catalysts varied in V/Ag ratios, ranging from 1/0 to 0/1. The intermediate V/Ag ratio catalysts before and after catalysis were mixtures of materials containing silver, vanadium, and oxygen. XRD, TEM, ESR, and FT-IR were used to characterize the catalysts before and after catalysis. The most selective catalysts for toluene oxidation to benzaldehyde were initially identified as the phases including $Ag_2V_4O_{10.84}$, $Ag_{1.2}V_3O_8$, and $AgVO_3$, with the optimal V/Ag ratio being 2.16.

In 1991, Vassileva et al. reported the complete air oxidation of benzene by SVO catalysts supported on Al_2O_3 [35]. Active catalyst material was prepared by combining $AgNO_3$ and NH_4VO_3 in ratios from 1:71 to 1:1 aqueous solution, the water was removed by heating, and the resulting material was calcined in air at 500–520°C. The catalysts were characterized via V^{5+}, V^{4+}, and V^{3+} composition (wt.%) as a function of catalysis time. In general, the V^{5+} composition decreased as the catalysis progressed, while the V^{4+} and V^{3+} compositions both increased. Samples prepared with initial silver to vanadium ratios of 1:71 and 1:19 were shown to exhibit the highest and most stable catalytic activity, whereas the 1:1 catalyst showed the lowest activity. The authors proposed that in order to optimize catalytic activity, an optimal V^{5+}/V^{4+} ratio was maintained when the silver was not chemically bound to the vanadium oxides and when a distinct phase of silver was not formed during catalysis.

In 1998 Zhang et al. followed up the 1991 report [34] (vide supra) by preparing V–Ag catalysts according to V/Ag ratios of 1/0, 9/1, 3/1, 2.16/1, 1.5/1, 1/1, and 0/1, and studying the reduction behavior of these materials via temperature programmed reduction in a H_2/N_2 atmosphere, X-ray diffraction, and ultraviolet diffuse reflectance spectra [36]. Reminiscent of the 1991 report, the catalysts were prepared by combining aqueous solutions of silver nitrate and ammonium metavanadate in the presence of a small amount of oxalic acid. The water was removed by evaporation and the dried product was calcined in a muffle furnace at 450°C for 9 h. Interestingly, the surface area of the products was largest with a V/Ag ratio = 1/0 and smallest with a V/Ag ratio = 0/1. The remaining products had surface areas which decreased as the V/Ag ratio decreased. The first step of reduction of $Ag_2V_4O_{11}$, $Ag_2V_4O_{10.84}$, and $Ag_{1.2}V_3O_8$ all formed Ag metal, V_6O_{13}, and H_2O. V_6O_{13} was then reduced to VO_2, which was then reduced to V_2O_3.

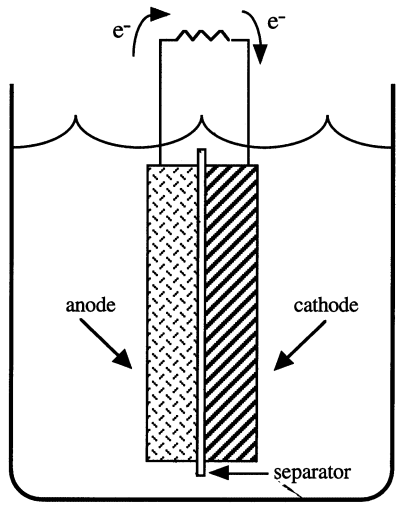

Fig. 4. A basic battery contains an anode, cathode, separator, and electrolyte. Electrons flow through load from anode to cathode.

3. Use of silver vanadium oxide in batteries

The basic components for a battery are illustrated in Fig. 4, and consist of an anode, a cathode, separator(s), and an electrolyte. Advanced batteries using lithium metal as the anode possess high energy density, expressed in terms of amp hours (Ah) or watt hours (Wh) per weight or volume of the battery. The high energy density of lithium batteries is due to the high electrochemical equivalence (or high coulombic output for a given weight of material) of lithium. Lithium metal has an electrochemical equivalence of 3860 mAh g^{-1} and a standard potential of -3.05 V at 25°C [37]. These values are the highest for any of the metals, and make lithium an excellent anode material. One limitation associated with lithium anode batteries is that due to the reactivity of lithium metal with water, these cells must utilize a nonaqueous electrolyte solution. The lower conductivity of organic-based electrolytes compared to aqueous electrolytes can limit the rate capability, or the level of current, a battery can provide. However, high performance lithium batteries have been designed which display utility in special applications where high power and high battery capacity are needed. It is in this area that SVO has found its niche as a cathode material for lithium batteries, and has been enthusiastically studied as such over the past two decades.

Commercially, it has been as a cathode material in a primary (non-rechargeable) lithium anode cell that SVO has made the largest impact, mainly associated with batteries for implantable medical devices. Specifically, lithium/SVO batteries are able to produce the high currents which are required for the operation of implantable cardiac defibrillators (ICDs) [38]. ICDs monitor the patient's heart and provide a high energy electrical shock to a patient experiencing ventricular fibrilla-

tion, which allows the heart to return to normal rhythm. In addition to meeting the technical requirements to power an ICD, the lithium/SVO battery has demonstrated the safety and reliability needed for an implantable battery. In 1991 Holmes and Visbisky reported on the reliability of SVO based cells used in implantable defibrillators [39]. A total of 788 cells were tested at 37°C under both constant resistive load and pulse discharge. Although none of the cells had reached premature end of test, a maximum random rate of failure of 0.0167% per month was calculated ($\alpha = 0.90$). Reliability and quality assurance programs for the construction of implantable grade lithium/SVO cells were also outlined by Takeuchi [40]. Data from the testing of over 3800 cells indicated a maximum random failure rate of 0.005% at a 90% confidence interval.

There have been several papers and patents related to the use of SVO as a high-rate cathode material for the ICD application. In addition to the high rate capability displayed by SVO as a cathode, this material also displays high energy density relative to other solid cathode materials used in lithium batteries (see Table 1). Additionally, there has also been interest in SVO and related materials as rechargeable cathode materials for lithium and lithium-ion type cells. Literature related to both of these intended applications are reviewed in the following sections.

3.1. Non-rechargeable silver vanadium oxide cells and cell design

In this section, the publications which focus on the use of SVO as a cathode material for advanced primary batteries will be reviewed.

The first reference to SVO as a cathode material for a battery occurred in 1978, where Scholtens and coworkers investigated various silver vanadium bronzes of the formula $Ag_xV_2O_5$ over a range of x values [41]. A solid electrolyte cell of the type: Ag/Ag-β-alumina/$Ag_xV_2O_5$ was devised, where silver metal was used as the anode and $Ag_xV_2O_5$ as the cathode. Galvanic cell measurements were then used to calculate the partial thermodynamic enthalpic and entropic functions of silver

Table 1
The gravimetric capacity of cathode materials used in lithium and lithium ion batteries tabulated from the literature

Cathode material	Capacity (mAh g^{-1})
CF_x	860 [77]
SVO ($Ag_2V_4O_{11}$)	315 [52]
MnO_2	308 [78]
TiS_2	226 [79]
$LiMoO_2$	199 [79]
$LiNiO_2$	160 [80]
$LiNi_{0.5}Co_{0.5}O_2$	147 [80]
$LiCoO_2$	131 [80]
$LiMn_2O_4$	123 [80]
$LiWO_2$	120 [79]

within the compound as x increased in 0.1 increments from 0.1 to 0.7. Attempts to measure the functions at lower values of x failed, but conductivity was measured in the region where $0.29 < x < 0.41$. This region was denoted the β phase, and was determined to be most stable from the thermodynamic measurements. With the benefit of hindsight, it is interesting to note that the authors commented that $Ag_xV_2O_5$ bronzes (in conjunction with a silver ion electrolyte) offered no possibilities for practical storage cells.

History began for the lithium/SVO cell in 1982, when Liang et al. were granted the first of two US patents for the use of metal vanadium oxides as cathodes in electrochemical cells [42]. The patent covered vanadium oxides reacted with several elements, including silver, via thermal decomposition reactions. The use of $Ag_2V_4O_{11}$ as a cathode in a lithium battery with a nonaqueous liquid electrolyte was disclosed by this patent, and the system was originally targeted for high temperature (ca. 150°C) battery application.

The first reference to the potential application of Li/SVO batteries for medical devices appeared in 1984, when Keister et al. proposed the use of lithium SVO based systems to power implantable devices [43]. The SVO material was designated as AgV_2O_5 in this paper, although the actual elemental analysis indicated a formula of $AgV_2O_{5.5-6.0}$, suggesting that the material was actually the ε-phase of SVO ($Ag_2V_4O_{11}$). The electrochemical cell consisted of SVO cathode, lithium anode, and 1M $LiBF_4$ electrolyte salt in propylene carbonate. The cell construction included a central lithium anode surrounded by a cathode. This cell design limited the area of contact between the electrodes and thus limited the rate capability of the cell. Pulse testing was limited to 10 mA, or 0.8 mA cm^{-2} of electrode area. While the low conductivity of the liquid electrolyte chosen for this cell ($LiBF_4$/propylene carbonate) also limited the rate capability of the system, the high boiling point of the solvent provided the cell the ability to tolerate autoclave temperatures of around 125°C.

A major step concerning the use of Li/SVO cells in implantable cardiac defibrillators was taken in 1986, when Keister et al. detailed the first implantable grade commercial cell based on SVO chemistry [44]. The system employed $Ag_2V_4O_{11}$ cathode material with a liquid organic electrolyte and lithium anode, all contained in a prismatic-shaped hermetically sealed stainless steel case. Extensive safety and performance testing was conducted on this cell, demonstrating the cell's ability to withstand abusive conditions as well as the ability to function at both low continuous currents and high current pulsitile loads. The cell was pulse tested using 2 A pulse currents, considerably higher than the 10 mA pulse testing conducted in the previous study. The large increase in rate capability of this cell was due in part to the use of a multi-plate cell design (see Fig. 5). By connecting several cathode plates in a parallel configuration, the effective surface area of the cathode was increased, allowing higher currents to be drawn from the cell.

In 1986, Takeuchi et al. further detailed the performance of the lithium/SVO system under high current discharge conditions [45]. In this reference, another piece of the puzzle concerning the high rate capability of this system was revealed. While the multiple electrode design accounted for some of the increased rate capability of

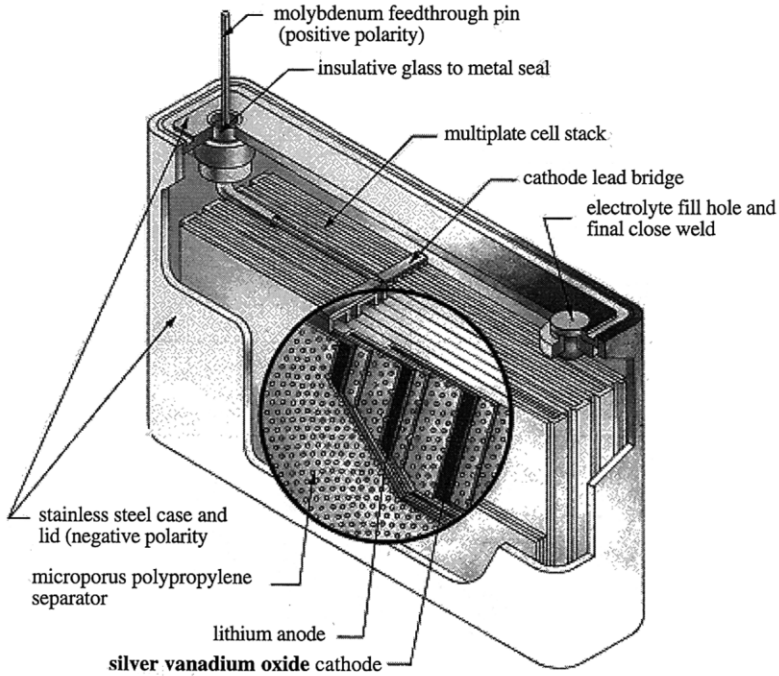

Fig. 5. A cutaway view of a silver vanadium oxide based primary cell manufactured by Wilson Greatbatch Ltd., Clarence, NY (shows flat plate type construction © 2000, Wilson Greatbatch Ltd. used with permission.)

these cells, the ratio of pulse current to electrode surface area was still much higher than that of previous lithium/SVO batteries. In this study up to 76% of theoretical capacity was obtained when the cell was discharged using pulses of 20 mA cm^{-2} of cathode area. A key behind this high rate capability was the development of nonaqueous electrolyte with high conductivity and good stability toward the anode and cathode materials. A lithium salt ($LiSO_3CF_3$ or $LiAsF_6$) in a 50:50 mix of propylene carbonate and dimethoxyethane was used for this system. In 1987, Holmes et al. also reported on the performance of this newly developed cell [46].

Recent innovations in implantable grade lithium/SVO batteries include the use of a wound-electrode design. In 1995 and later in 1997, Crespi et al. [47] and Skarstad [48] (respectively) reported on the design of a SVO cathode fashioned into a spirally wound electrode assembly. The crystalline SVO material was prepared via a combination reaction, and was characterized via high-resolution transmission electron microscopy and X-ray diffraction. The cell was capable of consuming 6.67 equivalents of lithium per $Ag_2V_4O_{11}$ formula unit. A spirally wound lithium/SVO cell was also described in 1998 by Takeuchi et al. [49]. This cell achieved a volumetric energy density of 540 Wh l^{-1}, delivered greater than 50% of theoretical capacity under loads greater than 3 Ω, and was successfully pulse discharged at 2.0

A. Several safety tests were conducted, including short circuit, forced overdischarge, crush and charging tests. It was reported that these cells did not rupture, vent, or leak under the abusive conditions.

3.2. Materials studies of silver vanadium oxide cathodes

This section reviews the materials chemistry of SVO as related to its use as a cathode material for advanced non-rechargeable batteries.

The choice of $Ag_2V_4O_{11}$ as cathode material for lithium cells was discussed in a paper by Takeuchi and Piliero in 1987 [50]. The authors prepared SVO cathode materials with silver to vanadium ratios of 0.01 to 1.0 via thermal decomposition of silver nitrate and vanadium pentoxide mixtures. Lithium anode batteries were built using the materials, and the batteries were discharged under several different loads. Cathodes containing primarily V_2O_5 gave the lowest capacity. The delivered capacity of the material with the formula $Ag_2V_4O_{11}$ was highest, while material containing mainly $AgVO_3$ was significantly lower. The $Ag_2V_4O_{11}$ cathodes also provided the lowest resistance under pulsed discharge conditions of any of the materials tested. Chemical lithiation of the cathode materials using *n*-butyllithium was conducted, and these experiments indicated that $Ag_2V_4O_{11}$ provided the highest theoretical volumetric energy density, in agreement with the actual electrochemical cell data. It is interesting to note that very different discharge curves were observed for the different cathode materials (see Fig. 6). Since the voltage of the lithium metal anode is nearly constant during discharge, the cathode plays a dominant role in determining the voltage of the cell as the battery is drained. The dependence of the cell voltage on the ratio of silver to vanadium in the cathode of these cells illustrates the differences in electrochemical behavior displayed by the different phases of SVO.

The electrochemical reduction of SVO during discharge of $Li/Ag_2V_4O_{11}$ cells was explored in greater detail by Takeuchi and Thiebolt in 1987. In this work they

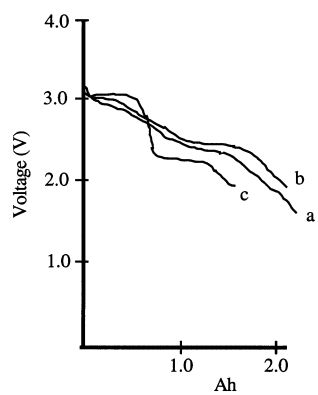

Fig. 6. Dependence of cell voltage on cathode composition as illustrated by discharge of $Ag_{0.76}V_2O_y$. (a) AgV_2O_y; (b) $Ag_2V_2O_y$; (c) against lithium [51].

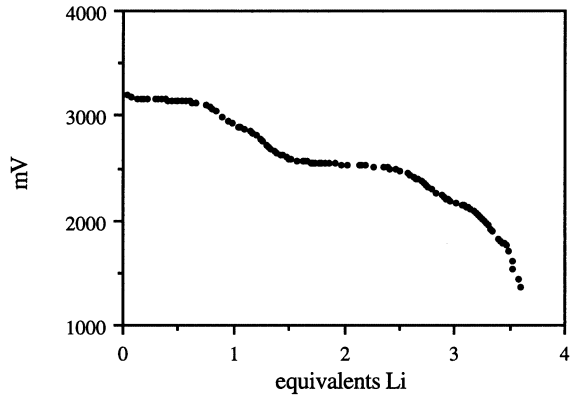

Fig. 7. A typical discharge curve is shown for a lithium silver vanadium oxide cell under constant resistive load [52,53].

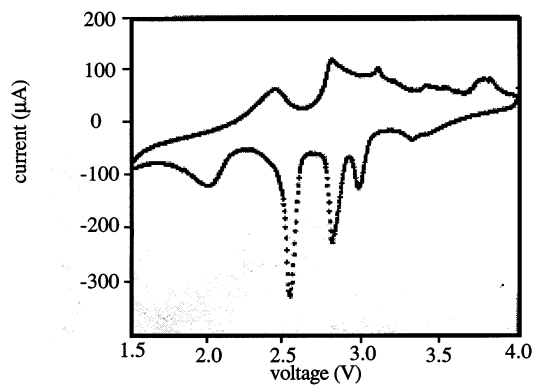

Fig. 8. Cyclic voltammetry of $Ag_2V_4O_{11}$ versus lithium conducted at 0.08 mV s^{-1} [53].

identified five voltage plateaus throughout the electrochemical discharge of SVO (see Fig. 7) [51,52]. To investigate the cathode composition at each plateau region, $Li/Ag_2V_4O_{11}$ cells were discharged to various stages and disassembled.

Coupled with the electrochemical characterization, chemical titration and atomic absorption were used to reveal the total amount and oxidation state of the silver and vanadium present in each sample. Most notably, low rate cyclic voltammetry on lithium/SVO was reported for the first time in this paper (see Fig. 8). Electrodes were prepared using the $Ag_2V_4O_{11}$ analyte, graphite conductive additive, and polyacrylic acid as binder. A low scan rate, 0.08 mV s^{-1}, was used for this experiment, resulting in well-resolved peaks in the voltammogram.

Starting in 1993, several published reports appeared which examined in greater detail the influence of the synthesis method of $Ag_2V_4O_{11}$ on the performance of cells using this cathode material. Leising and Takeuchi studied the effects of synthesis temperature on SVO [53]. The reaction of $AgNO_3 + V_2O_5$ was used to prepare

$Ag_2V_4O_{11}$ at temperatures of 320, 375, 450 and 540°C. A key difference identified in these materials was that the morphology of the material prepared at 450°C was much different than the samples prepared at 320 and 375°C. While the materials prepared at lower temperature displayed irregularly-shaped particles, the 450°C material displayed small nanoscale (< 1 μm in diameter) needlelike particles. Although the results of a rapid discharge test were very similar for cathodes containing materials prepared at 320 to 450°C, the physical characterization indicated that the temperature of synthesis played an important role in determining the properties of the solid product. The material prepared at 540°C was found to be very different from all of the other materials. At 540°C the $Ag_2V_4O_{11}$ material began to soften, and on cooling yielded large plate-like particles, which contained a mixture of phases.

In 1993, Crespi was granted a US patent for electrochemical cells constructed with SVO cathodes prepared via an addition reaction of $AgVO_3$ or Ag_2O with V_2O_5 [54]. The inventor maintained that the chemical addition reaction conducted at 520°C produced $Ag_2V_4O_{11}$ which electrochemically performed differently than material prepared by the method outlined by Liang in the 1982 patent [42]. The $Ag_2V_4O_{11}$ material described by Liang was prepared at 360°C by a thermal decomposition of $AgNO_3$ and V_2O_5. It was shown that the cathode material prepared by chemical addition at 520°C displayed higher rate capability than the 360°C thermal decomposition material, when test cells were pulsed using current

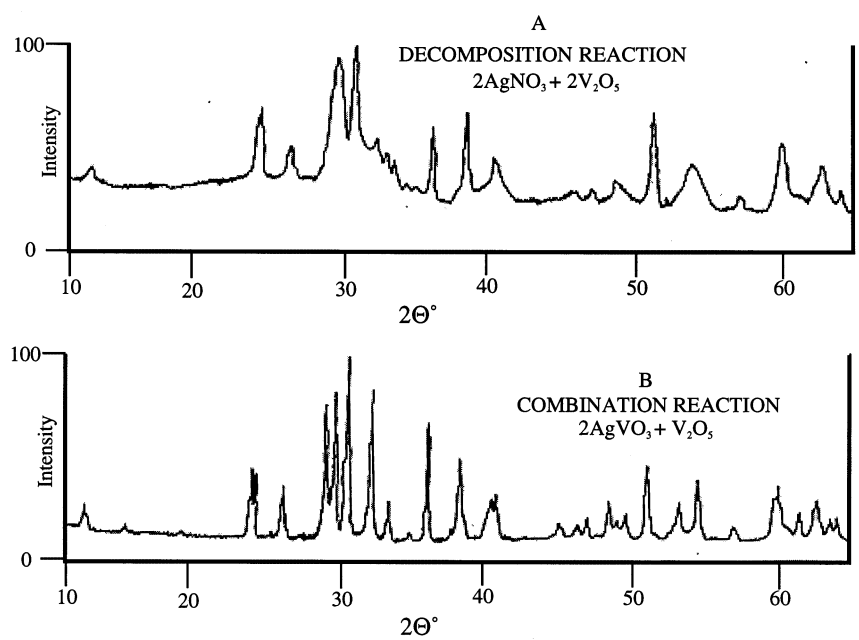

Fig. 9. X-ray powder diffraction pattern shown for $Ag_2V_4O_{11}$ samples prepared by: (a) chemical addition at 520°C and (b) thermal decomposition at 360°C [55].

densities of 12 or 19 mA cm^{-2}. The 520°C chemical addition material also displayed greater crystallinity, as measured by X-ray powder diffraction (see Fig. 9), than the 360°C thermal decomposition material.

In 1994 Leising and Takeuchi investigated the synthesis of SVO under both air and argon at 500°C from several silver precursors including silver nitrate, silver nitrite, silver vanadate, silver oxide, silver carbonate, and silver metal [28]. Materials prepared under air at the same temperature using either the thermal decomposition reaction ($AgNO_3$) or the chemical addition reaction (Ag_2O or $AgVO_3$) appeared similar in terms of morphology, crystallinity, thermal properties, and electrochemical performance. Interestingly, the crystallinity of the $Ag_2V_4O_{11}$ synthesized at 500°C by the thermal decomposition reaction was actually higher than the $Ag_2V_4O_{11}$ prepared at 500°C by the chemical addition reaction, as illustrated by X-ray powder diffraction patterns (see Fig. 10). The increased crystallinity of $Ag_2V_4O_{11}$ prepared at higher temperature (500–520°C) via the thermal decomposition route is reiterated in a 1999 US Patent issued to Crespi and Chen [55]. In this patent the inventors claim the use of $Ag_2V_4O_{11}$ prepared by the thermal decomposition route at 360°C, according to the Liang method, which is then reheated to a higher temperature to give a more crystalline material.

Further characterization of the SVO discharge reaction in lithium batteries was published by Leising et al. in 1994 [56]. In this study $Li_xAg_2V_4O_{11}$ products were prepared and isolated over the range of $0 < x < 6.6$. A combination of physical and wet chemical characterization techniques were used to identify the composition of the product cathode materials. X-ray powder diffraction experiments demonstrated that the reduction of SVO in the process $Li + Ag_2V_4O_{11} \rightarrow Li_xAg_2V_4O_{11}$ resulted in

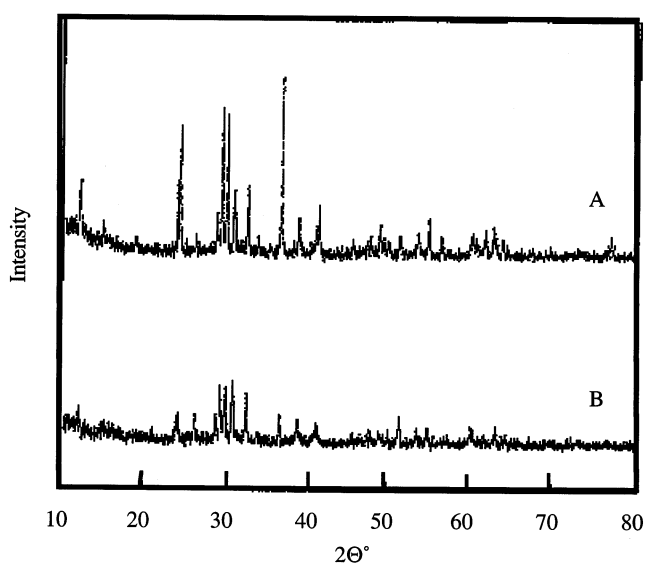

Fig. 10. X-ray diffraction pattern shown for $Ag_2V_4O_{11}$ samples prepared by: (a) thermal decomposition at 500°C and (b) chemical addition at 500°C [56].

a loss of crystallinity over the range $0 < x < 2.4$, with the concurrent reduction of Ag^+ to Ag^0. The reduction of silver to the metallic form was found to play an important role in the battery chemistry. First, it accounted for ca. 30% of the overall capacity of the cathode material, and additionally the formation of metallic silver was found to greatly increase the conductivity of the cathode material. Resistivity measurements of discharged cathode samples displayed a five-orders of magnitude reduction in resistivity between the starting $Ag_2V_4O_{11}$ and the material containing reduced silver. The enhanced conductivity of the reduced cathode material contributes to the high rate capability displayed by the lithium/SVO system, which is a key property of the material. At x values > 2.4 in $Li_xAg_2V_4O_{11}$ the reduction of V^{5+} to V^{4+} and V^{3+} was identified. It was found that the reduction of V^{4+} to V^{3+} competed with the reduction of V^{5+} to V^{4+} at $x > 3.8$, resulting in the formation of mixed-valent materials, where vanadium(III), (IV) and (V) were found in the same sample.

In 1995, Crespi et al. used high resolution electron microscopy to investigate the structure of slightly silver-deficient $Ag_{2-y}V_4O_{11}$ [57]. During the discharge reaction using this material as a cathode, silver particles were observed on the outside of the needle-shaped SVO particles, which confirmed that the first step in the lithiation of this material was reduction of silver. The stacking of the vanadium oxide layers was also found to become random in this process.

Other modifications to the synthesis of SVO cathode material have been reported. In 1995, Takeuchi and Thiebolt patented a new preparation for SVO cathodes prepared via addition of elemental silver to vanadium compounds present in an anhydrous mixture. Oxygen deficient SVO compounds were found, as well as compounds designed to provide a desired shape in the electrical discharge curve of the cell [58]. Following this work in 1996, Takeuchi and Thiebolt patented several methods for the preparation of amorphous SVO prepared by chemical addition reaction at temperatures high enough to melt the mixture, coupled with rapid cooling [59]. The use of a phosphorus pentoxide dopant was also discussed.

3.3. Electrochemical studies of primary silver vanadium oxide cells

Following the initial description of the technology in 1986, the detailed electrochemical characterization of the lithium/SVO battery system continued in several publications. Bergman et al. presented calorimetric analysis of lithium/SVO cells in 1987 [60]. Heat dissipation during cell discharge was characterized under several resistive loads, where these experiments were undertaken to determine the long-term stability of the cells. Although calorimetric measurements suggested a self discharge rate as high as 3.4% per year, analysis of residual lithium present after discharge suggested that the actual self discharge rate was less than 1% per year. Heat dissipation due to cell polarization and entropy were determined to be small, and the difference was attributed to parasitic side reactions of lithium and non-Faradaic contributions.

In 1988, Takeuchi et al. measured the diffusion rate of lithium in SVO electrodes [61]. Cells were discharged to various depths of discharge, allowed to equilibrate,

and then pulsed. From the pulse data, voltage recovery times were used to determine lithium diffusion rates. It was found that the rate and magnitude of voltage recovery after high rates of discharge was not constant at all depths of discharge. These results suggested that the electrochemical characteristics of SVO change as the material is reduced. In 1989, Bergman and Takeuchi investigated the complex impedance characteristics of lithium/SVO cells [62]. Complex impedance responses were generated at various levels of discharge, and the cells were repeatedly stored and then pulsed to determine voltage delay. Voltage delay refers to an initial drop in voltage when a cell is subjected to a pulsitile discharge after a long storage period. Subsequent pulses are not expected to show the same voltage drop. Voltage drops of 850–905 mV were recorded in this study, with 100–150 mV due to voltage delay.

Low temperature performance of the lithium/SVO batteries was investigated in 1990 by Takeuchi et al. [63], to characterize this system for possible nonmedical specialty applications. Twenty-three percent of theoretical capacity was obtained under constant resistive load at -40°C, and seventy percent theoretical capacity at 0°C. Under pulsitile discharge, 40% of theoretical capacity was obtained at -40°C. In addition to the electrochemical testing, cells were safety tested under short circuit and crush conditions. The crush testing was designed to generate an internal short circuit, and no violent cell behavior was observed. The peak temperature on crush test was 60°C, while on external short circuit the cells reached 80–130°C.

In another paper detailing the electrochemical characterization of implantable grade batteries, Takeuchi and Thiebolt in 1991 investigated the nature and mechanism of lithium deposition inside sealed Li/SVO cells [64]. It was found that small clusters of lithium metal could deposit on non-active components inside the cell during discharge. To investigate this process, case neutral cells were constructed, and the current flow between the case and anode was measured following intermittent high current discharges. This current was correlated with the amount of deposited lithium measured via destructive analysis of the cell. This study concluded that inhomogeneous discharge of the cathode under high rates could induce lithium deposition. It was also found that cell orientation during discharge, current level, and frequency of pulse discharge play an important role in determining the amount of lithium deposited.

In 1993, Crespi and Skarstad investigated parasitic reactions in lithium/SVO cells [65]. Using microcalorimetry the reaction rate was directly related to anode surface area and was estimated to occur at 0.65 mAh cm^{-2} per year. A system of nonlinear equations was proposed to take into account these reactions when designing lithium/SVO cells. In 1997, Norton and Schmidt investigated the internal resistance of lithium–SVO cells [66]. Internal resistance was measured as a function of current density, pulse duration, and depth of discharge. At lower current densities and pulse duration, ohmic components dominate resistance. However, at higher pulse amplitudes and lengths, mass transfer limitations result in rapidly increasing internal resistance.

In 1999, Gan and Takeuchi identified a key role of anode surface film composition in SVO cell performance [67]. The addition of carbon dioxide synthons such as

dibenzyl carbonate and benzyl succinimidyl carbonate was found to alleviate voltage delay and resistance build-up in silver vanadium oxide cells.

3.4. Rechargeable silver vanadium oxide cells

The use of SVO as a rechargeable cathode material is enticing due to the high energy density (>300 mAh g^{-1}) of this material. However, during the discharge reaction of a lithium/SVO cell, the reduced silver is replaced by lithium in the vanadium oxide matrix. The reversibility of this lithium for silver substitution under charge conditions is still a matter of debate, as will be outlined below.

In 1991 Takada et al. investigated the reversibility of silver intercalation in silver vanadium bronzes ($Ag_xV_2O_5$), where materials were prepared with x in the range $0.3 < x < 1.0$ [68]. Silver ion conductive solid electrolytes were used to study the electrochemistry of the materials against a silver powder anode. From the electrochemical tests, it was found that the δ-phase ($0.67 \leqslant x \leqslant 0.86$) material was electroactive, while the β-phase ($0.29 \leqslant x \leqslant 0.41$) was not. Characterization of the silver vanadium bronzes obtained by electrochemical intercalation and deintercalation of silver was accomplished by X-ray diffraction. It was proposed that new phases of SVO were obtained by the electrochemical reaction, which were structurally distinct from those synthesized at high temperature. Rechargeable cells were fashioned using $Ag_{0.7}V_2O_5$ for both the anode and the cathode, with $Ag_6I_4WO_4$ as the solid state electrolyte. By using twice as much $Ag_{0.7}V_2O_5$ in the anode as the cathode, the battery was configured such that the silver composition would vary between 0.81 and 0.90 for x in $Ag_xV_2O_5$ in the anode, and 0.30 and 0.47 for x in $Ag_xV_2O_5$ for the cathode. This produced a cell with a running voltage between 0.5 and 0.25 V, which was charged and discharged (cycled) over 600 times. However, it should be noted that aside from the low voltage produced by the cell, the capacity of the cathode was found to be only 5 to 10 mAh g^{-1}.

In 1992, Garcia-Alvarado et al. reported that the δ-phase silver vanadium bronze $Ag_{0.68}V_2O_5$ could be used as a starting material to produce cathode materials for rechargeable lithium batteries [69]. In this study δ-$Ag_{0.68}V_2O_5$ was reacted with NO_2BF_4 oxidizing agent to remove silver and form the new materials: $Ag_xV_2O_5$ with $x = 0.4$, 0.15, and 0.04. Cells containing $Ag_xV_2O_5$ cathodes with $x = 0.68$ and 0.4 incorporated 2.9 and 2.7 equivalents of lithium, respectively, on the first discharge. In comparison, cells using cathodes containing lower silver contents ($x = 0.15$ and 0.04) displayed large polarization, decreased initial capacities of 2.3 and 2.1 equivalents of lithium, and large decreases in capacity on the second cycle.

In a later paper, Tarascon and Garcia-Alvarado also prepared the vanadates $Ag_2V_4O_{11}$ and $Ag_2V_4O_{11-y}$ and studied the intercalation and deintercalation of lithium into these compounds [29]. Multiple phases were observed and characterized during charge and discharge of the samples between 3.6 V and 1.5 V. The formation of $Li_xAg_2V_4O_{11}$ was characterized as reversible over the range of $0 \leqslant x \leqslant 7$, although the replacement of silver by lithium from $0 \leqslant x \leqslant 2$ was reported as irreversible. The oxygen deficient material, $Ag_2V_4O_{11-y}$, was found to incorporate a maximum of 5.7 equivalents of lithium, yielding a lower capacity. As

in the earlier study, oxidation of the SVO starting material by NO_2BF_4 was used to produce new cathode materials with decreased silver contents. These new cathode materials all displayed a maximum capacity of 5.7 Li per unit formula, similar to the oxygen deficient material.

In 1995, West and Crespi studied the reversibility of the lithium insertion process in $Ag_2V_4O_{11}$ [70]. A polymer electrolyte $Li/Ag_2V_4O_{11}$ cell was tested at 100°C between 2.2 and 3.5 V via X-ray diffraction and cyclic voltammetry. The formation of metallic silver was identified in the X-ray diffraction patterns for the reduced cathodes, consistent with the earlier findings of Leising et al. [56] and Garcia-Alvarado et al. [29]. However, this study also showed that at high temperature (100°C) some reversible formation of $Ag_2V_4O_{11}$ takes place at the cathode when charged to 3.5 V. It was proposed that silver was oxidized and re-entered the vanadium oxide matrix upon charge. Based on the shape of the charge/discharge curves for a $Li/Ag_2V_4O_{11}$ cell using propylene carbonate liquid electrolyte at 25°C, the authors maintained that silver also re-inserts into the vanadium oxide framework at ambient temperatures. The reversibility of the $Li/Ag_2V_4O_{11}$ system was poor, where 80% capacity fade was reported for 25 cycles when the system was charged to 3.5 V, and 45% capacty fade for 25 cycles when charged to 3.25 V. Capacity fade is defined as the percent loss of capacity during cycling as compared to the starting capacity of the cell.

Kawakita et al. investigated the performance of $Ag_{1+x}V_3O_8$ cathode material [71], prepared via an exchange reaction of $Na_{1+x}V_3O_8$ with Ag^+ ions or the solid state reaction of Ag_2O and V_2O_5. Discharge of the material against a lithium anode resulted in displacement of the silver ions and their reduction to silver metal upon discharge. In contrast to the work of West [70], however, oxidation and reinsertion of silver was not observed during charge. Silver metal was identified in X-ray diffraction patterns of the charged cathode, and no anodic peaks corresponding to $Ag(0) \rightarrow Ag(I)$ were observed in cyclic voltammetry of the system, confirming that silver was not returned to the vanadium oxide matrix.

Kawakita et al. also prepared layered sodium SVOs of the formula $(Na_yAg_{1-y})_2V_4O_{11}$ by substituting part of the silver ions in $Ag_2V_4O_{11}$ with sodium [72]. Discharge curves similar to that obtained with pure SVO were obtained, and reduction of Ag(I) was observed in competition with V(V) reduction. Unlike $Ag_2V_4O_{11}$, which becomes amorphous on discharge, $Na_{1.54}Ag_{0.46}V_4O_{11}$ still displayed X-ray diffraction corresponding to the starting material upon deep discharge to 2 V. This material was cycled successfully with less capacity loss than that observed with pure SVO, indicating the sodium may have stabilized the structure. The authors maintained that substituting some silver with sodium results in a pillar effect, in which sodium ions continue to connect adjacent layers in the material.

In 1998, Kawakita et al. studied the use of δ-AgV_2O_5 in rechargeable systems [73]. Approximately three equivalents of lithium were inserted into the material over three distinguishable voltage plateaus. In the first region, Ag(I) is reduced to Ag(0). In the second region, the δ-phase $Ag_yV_2O_5$ changes to ε-phase $Li_xV_2O_5$, and in the third region, additional lithium ions are inserted into the ε material. Once again, Ag(I) did not return to the vanadate on charge once Ag(0) was formed during discharge.

Coustier et al. has investigated reacting Ag(0) powder with vanadium pentoxide hydrogels to produce silver-doped vanadium oxides [74–76]. Mixtures of V_2O_5 hydrogels were vigorously mixed with silver powder until the silver was completely oxidized. The addition of a full equivalent of silver to vanadium oxide resulted in a material which displayed several X-ray diffraction peaks corresponding to those found in $Ag_2V_4O_{11}$. The addition of silver increased the V_2O_5 conductivity three-fold. Cathodes were constructed from the material and discharged against lithium, intercalating a maximum of four equivalents of lithium. No silver loss occurred during cycling. Samples of $Ag_{0.3}V_2O_5$ were shown to retain a capacity of over 250 mAh g^{-1} after 65 cycles at a C/4 rate.

The number of years between the publication of the first SVO papers and those published in the present day is quite long, and indicates that there is significant history associated with SVO research. Early papers reported the synthesis and characterization of the material, with particular emphasis on structural characterization of several different phases of SVO. Variations in reaction conditions, starting materials, and reagent stoichiometeries were found to result in the formation of many different products with varying properties. As an example of the materials available, in the presence of air, the combination of silver with vanadium oxides in different ratios yielded β ($Ag_{0.3}V_2O_5$), γ ($Ag_{1.12}V_3O_{7.8}$), and ε ($Ag_2V_4O_{11}$) phases as well as $AgVO_3$, $Ag_4V_2O_7$ and Ag_3VO_4. In addition, the combination of these starting materials in inert atmospheres yielded mainly different products. Materials of the general formula $Ag_xV_2O_5$ were found in this case, where the α phase ($0 \leqslant x \leqslant 0.01$), β phase ($0.29 \leqslant x \leqslant 0.41$), and δ phase ($0.67 \leqslant x \leqslant 0.86$) were characterized. Besides the physical characterization of SVO, there has also been several reports on the chemical reactivity of these materials. Some of these reports focused on the interconversion of phases with variation in temperature and atmosphere, while others reported the use of SVO as a catalyst for the oxidation of organic substrates. Taken together, the characterization of SVO materials in these earlier studies provided an important foundation for the successful commercial use of SVO.

The focus of much of the research on SVO shifted to the ε-phase when this material was discovered to be a useful cathode material for advanced lithium batteries. SVO was found to possess high rate capability and capacity as a cathode material, and Li/SVO batteries have since been commercially successful in powering implantable medical devices. The importance of this application and the key role played by the SVO cathode material has led to a large increase in the number of reports on SVO in recent years. Li/SVO batteries have demonstrated high reliability and safety, which has been documented in several references. Much of the work surrounding SVO cathode materials has also focused on the electrochemical characterization of the material, where lithiation of SVO has been analyzed and described in detail. Likewise, a number of synthetic routes to prepare SVO have been described in publications and patents to optimize the ability of the material to function as a primary cathode material. As an extension of the work on non-rechargeable Li/SVO batteries, several studies have also looked at the ability of SVO to act as a rechargeable cathode material. There is still some controversy in

the literature concerning the reversibility of silver oxidation/reduction in SVO during the charge and discharge of the material. This issue may require further study to bring agreement on the subject. Due to the complexity of SVO chemistry as well as the subtle and sometimes not well understood structural–functional relationships between the chemistry of SVO and the electrochemical performance parameters of batteries utilizing SVO electrodes, the future for SVO research remains bright.

References

[1] H.T.S. Briton, R.A. Robinson, J. Chem. Soc. Lond. (1930) 2328
[2] H.T.S. Briton, R.A. Robinson, J. Chem. Soc. Lond. (1933) 512
[3] I. Lukas, C. Strusievici, C. Liteanu, Z. Anorg. Allg. Chem. 349 (1967) 92.
[4] A. Casalot, Bull. Soc. Chim. 4 (1969) 1103.
[5] B.K. Chakraverty, M.J. Sienko, J. Bonnerot, Phys. Rev. B Solid State 17 (1978) 3781.
[6] L. Znaidi, N. Baffier, M. Huber, Mater. Res. Bull. 24 (1989) 1501.
[7] A. Casalot, M. Pouchard, Bull. Soc. Chim. 10 (1967) 3817.
[8] A. Deschanvres, B. Raveau, C R Acad. Sci. Paris 259 (1964) 3553.
[9] P. Fleury, R. Kohlmuller, M.G. Chaudron, C R Acad. Sci. Paris 262 (1966) 475.
[10] A. Casalot, H. Cazemajor, P. Hagenmuller, M. Pouchard, Bull. Soc. Chim. 1 (1968) 85.
[11] B.B. Scholtens, Mater. Res. Bull. 11 (1976) 1533.
[12] V.L. Volkov, A.A. Fotiev, N.G. Sharova, L.L. Surat, Russ. J. Inorg. Chem. 21 (1976) 1566.
[13] E. Wenda, J. Therm. Anal. 30 (1985) 879.
[14] Y.Y. Ivanova, Y.B. Dimitriev, Mater. Chem. Phys. 12 (1985) 397.
[15] S. Andersson, Acta Chem. Scand. 19 (1965) 269.
[16] S. Andersson, Acta Chem. Scand. 19 (1965) 1371.
[17] P. Hagenmuller, J. Galy, M. Pouchard, A. Casalot, Mater. Res. Bull. 1 (1966) 45.
[18] J. Galy, M. Pouchard, A. Casalot, P. Hagenmuler, Bull. Soc. Fr. Miner. Cristallogr. Sect. C (1967) 544.
[19] Y.N. Dorzdov, E.A. Kuzmin, N.V. Belov, Sov. Phys. Crystallogr. 19 (1974) 36.
[20] R. Enjalbert, J. Galy, Acta Crystallogr. Sect. C 42 (1986) 1467.
[21] J. Galy, J. Solid State Chem. 100 (1992) 229.
[22] E. Deramond, J.-M. Savariault, J. Galy, Acta Crystallogr. Sect. C 50 (1994) 164.
[23] P.Y. Zavlij, M.S. Whittingham, Acta Crystallogr. Sect. B 55 (1999) 627.
[24] A.M. Crespi, P.M. Skarstad, H.W. Zandebergen, J. Schoonman, Proc. Symp. Lithium Batt., Pennington, NJ, vols. 93–94, 1993, p. 98.
[25] H.W. Zandbergen, A.M. Crespi, P.M. Skarstad, J.F. Vente, J. Solid State Chem. 110 (1994) 167.
[26] P. Rozier, J.M. Savariault, J. Galy, J. Solid State Chem. 122 (1996) 303.
[27] P. Rozier, J. Galy, J. Solid State Chem. 134 (1997) 294.
[28] R.A. Leising, E.S. Takeuchi, Chem. Mater. 6 (1994) 489.
[29] F. Garcia-Alvarado, J.M. Tarascon, Solid State Ionics 73 (1994) 247.
[30] P. Rozier, J.M. Savariault, J. Galy, Mater. Res. Soc. Symp. Proc. 575 (2000) 113.
[31] B. Raveau, Rev. Chim. Min. 4 (1967) 729.
[32] R.I. Andreikov, V.L. Volkov, Trans. Kinetika Katlitz 4 (1981) 963.
[33] J. Van Den Berg, A. Broersma, A.J. Van Dillen, J.W. Geus, Thermochim. Acta 63 (1983) 123.
[34] H. Zhang, W. Zhong, X. Xiang, X. Fu, J. Catal. 129 (1991) 426.
[35] M. Vassileva, A. Andreev, S. Dancheva, Appl. Catal. 69 (1991) 221.
[36] X. Ge, H. Zhang, J. Solid State Chem. 141 (1998) 186.
[37] D. Linden, in: D. Linden (Ed.), Handbook of Batteries and Fuel Cells, McGraw-Hill, New York, 1984, pp. 11.5–11.6.
[38] J.P. Nelson, Proc.12th Int. Semin. Prim. and Sec. Batt., Deerfield Beach, FL, 6–9 March, 1995.

[39] C. Holmes, M. Visbisky, Pace 14 (1991) 341.
[40] E.S. Takeuchi, J. Power Sources 54 (1995) 115.
[41] B.B. Scholtens, R. Polder, G.H.J. Broers, Electrochim. Acta 23 (1978) 483.
[42] C.C. Liang, E. Bolster, R.M. Murphy, United States Patent 4 310 609 (1982).
[43] P. Keister, R.T. Mead, S.J. Ebel, and W.R. Fairchild, Proc. 31st Int. Power Sources Symp., Pennington, NJ, 1984, pp. 331–338.
[44] P.P. Keister, E.S. Takeuchi, C.F. Holmes, Cardiostim 86 (1986) abstr. no. 463.
[45] E.S. Takeuchi, M.A. Zelinsky, and P. Keister, Proc. 32nd Int. Power Sources Symp., Pennington, NJ, 1986, pp. 268–273.
[46] C.F. Holmes, P. Keister, E.S. Takeuchi, Prog. Batt. Solar Cells 6 (1987) 64.
[47] A.M. Crespi, F.J. Berkowitz, R.C. Buchman, M.B. Ebner, W.G. Howard, R.E. Kraska, P.M. Skarstad, in: A. Attewell, T. Keily (Ed.), Power Sources 15, Alan Sutton Publishing Ltd., Stroud, UK, 1995, pp. 349–357.
[48] P.M. Skarstad, Proc. 12th Annual Battery Conf. App. Adv., Los Angeles, CA, 1997, pp. 151–155.
[49] E.S. Takeuchi, R.T. Mead, Proc. 33rd Int. Power Sources Symp., Pennington, NJ, 1988, pp. 667–675.
[50] E.S. Takeuchi, P. Piliero, J. Power Sources 21 (1987) 133.
[51] W.C. Theibolt, E.S. Takeuchi, Ext. Ab. Batt. Div. Electrochem. Soc. 87-2 (1987) 29.
[52] E.S. Takeuchi, W.C. Thiebolt, J. Electrochem. Soc. 135 (1988) 2691.
[53] R.A. Leising, E.S. Takeuchi, Chem. Mater. 5 (1993) 738.
[54] A.M. Crespi, United States Patent 5 221 453 (1993).
[55] A.M. Crespi, K. Chen, United States Patent 5 955 218 (1999).
[56] R.A. Leising, W.C. Theibolt, E.S. Takeuchi, Inorg. Chem. 33 (1994) 5733.
[57] A.M. Crespi, P.M. Skarstad, H.W. Zandbergen, J. Power Sources 54 (1995) 68.
[58] E.S. Takeuchi, W.C. Thiebolt, United States Patent 5 389 472 (1995).
[59] E.S. Takeuchi, W.C. Thiebolt, United States Patent 5 498 494 (1996).
[60] G.M. Bergman, S.J. Ebel, E.S. Takeuchi, P. Keister, J. Power Sources. 20 (1987) 179.
[61] E.S. Takeuchi, W.C. Thiebolt, Ext. Ab. Batt. Div. Electrochem. Soc. 88-2 (1988) 47.
[62] G.M. Bergman, E.S. Takeuchi, J. Power Sources 26 (1989) 365.
[63] E.S. Takeuchi, D.R. Tuhovak, C.J. Post, Proc. 34th Int. Power Sources Symp., New York, NY, 1990, pp. 355–358.
[64] E.S. Takeuchi, W.C. Thiebolt, J. Electrochem. Soc. 138 (1991) L44.
[65] A.M. Crespi, P.M. Skarstad, J. Power Sources 43-44 (1993) 119.
[66] J.D. Norton, C.L. Schmidt, Electrochem. Soc. Proc. 97-18 (1997) 389.
[67] H. Gan, E. Takeuchi, Ext. Ab. Batt. Div. Electrochem. Soc. 99-2 (1998) 332.
[68] K. Takada, T. Kanbara, Y. Yamamura, S. Kondo, Eur. J. Solid State Inorg. Chem. 28 (1991) 533.
[69] F. Garcia-Alvarado, J.M. Tarascon, B. Wilkens, J. Electrochem. Soc. 139 (1992) 3206.
[70] K. West, A.M. Crespi, J. Power Sources 54 (1995) 334.
[71] J. Kawakita, Y. Katayama, T. Miura, T. Kishi, Solid State Ionics 99 (1997) 71.
[72] J. Kawakita, K. Makino, Y. Katayama, T. Miura, T. Kishi, J. Power Sources 75 (1998) 244.
[73] J. Kawakita, H. Sasaki, M. Eguchi, T. Miura, T. Kishi, J. Power Sources 70 (1998) 28.
[74] F. Coustier, S. Passerini, W.H. Smyrl, Solid State Ionics 100 (1997) 247.
[75] F. Coustier, J. Hill, S. Passerini, W.H. Smyrl, Electrochem. Soc. Proc. 98-16 (1998) 350.
[76] F. Coustier, S. Passerini, J. Hill, W.H. Smyrl, Mater. Res. Soc. Symp. Proc. 496 (1988) 353.
[77] D. Linden, in: D. Linden (Ed.), Handbook of Batteries and Fuel Cells, McGraw-Hill, New York, 1995, p. 14.59.
[78] D. Linden, in: D. Linden (Ed.), Handbook of Batteries and Fuel Cells, McGraw-Hill, New York, 1995, p. 1.8.
[79] S. Hossain, in: D. Linden (Ed.), Handbook of Batteries and Fuel Cells, McGraw-Hill, New York, 1995, p. 36.4.
[80] D. Huang, Adv. Battery Technol. 11 (1998) 21–23.